Polymer 50 (2009) 5499–5507

Contents lists available at ScienceDirect

Polymer

journal homepage: www.elsevier.com/locate/polymer

Influence of e-beam irradiation on the dynamic creep and fatigue properties of poly(aliphatic/aromatic-ester) copolymers for biomedical applications

C. Götz [a], U.A. Handge [a], M. Piatek [b], M. El Fray [b], V. Altstädt [a,*]

[a] Department of Polymer Engineering, Faculty of Engineering Sciences, University of Bayreuth, Universitätsstrasse 30, 95447 Bayreuth, Germany
[b] Division of Biomaterials and Microbiological Technologies, Szczecin, West Pomeranian University of Technology, ul. Pulaskiego 10, 70-32 Szczecin, Poland

ARTICLE INFO

Article history:
Received 5 February 2009
Received in revised form
10 September 2009
Accepted 18 September 2009
Available online 22 September 2009

Keywords:
Thermoplastic elastomers
E-beam irradiation
Hysteresis measurements

ABSTRACT

Biomaterials must meet special medical prerequisites like biocompatibility and resistance to degradation and fracture, especially under cyclic loading. Promising candidates are poly(aliphatic/aromatic-ester) (PED) multiblock copolymers, which belong to the class of thermoplastic elastomers (TPEs), characterized by a physical network of semi-crystalline hard segments. Here we focus on the dynamic creep and fatigue performance of these TPEs and compare their behaviour with commercial benchmark materials. The PEDs were e-beam cured, to enhance their fatigue behaviour by the formation of an additional network structure. All materials were evaluated using quasi-static tensile tests and dynamic hysteresis measurements. Their mechanical properties were related to the network structure. E-beam irradiation increased the tensile strength and decreased the dynamic creep rate of PEDs. This effect can be explained by the formation of chemical cross-links, which are located in the hard phase segments. In conclusion, these novel biomaterials are a comparable alternative to their commercial counterparts like silicones and thermoplastic polyurethanes.

1. Introduction

Thermoplastic elastomers (TPE) constitute a relatively new group of polymeric materials which can be classified as a separate category of rubbers. TPEs do not need to be vulcanized and therefore offer many advantages in comparison to chemically cross-linked elastomers, while being processible as conventional thermoplastics. High performance TPEs with a good solvent resistance, elasticity, tear strength and flex fatigue properties are used in a wide range of medical applications such as medical tubing or equipment parts [1].

Because of their chemical structure and the matrix-domain morphology, characterized by the presence of hard and soft segments, selected TPEs like poly(ether–urethanes) or poly(ester–ether)s have unique physiochemical and mechanical properties and show a high degree of biocompatibility [2]. These TPEs are commonly used for medical implant applications as well as silicone and thermoplastic urethanes [1,3,4].

The mechanical behaviour of biomaterials like implants or rubbery medical parts is as important as their biocompatibility since an inadequate performance or even premature failure can let to health issues for patients. Therefore the durability or long-term mechanical behaviour of new biomaterials has become a prime concern in their adoption for medical devices. In addition, most of the loadings during the use as a body implant are dynamical in nature and polymers are known to creep or relax under sustained loadings. Implants should remain in the body for a long time [5], such that the number of surgical operations on patients is reduced, In order to evaluate the long-term dynamic properties of potential biomaterials a dynamic sinusoidal loading can be applied to the material specimen at various step-wise increasing load intervals. This step-wise increasing load test (SILT) induces a progressive deterioration of dynamic properties of the materials [6,7].

Recently novel poly(aliphatic/aromatic-ester)s (PEDs) have been synthesized as an alternative biomaterials for temporary flexor tendon prosthesis [8]. These PEDs contain discrete (nanometric) hard segments of semi-crystalline poly(butylene terephthalate) (PBT) embedded in a matrix of soft segments containing aliphatic dimer fatty acid, here dilinoleic acid (DLA) that impart the elastomeric character to the copolymer. The DLA component has a good oxygen and thermal stability and is suitable for biomedical applications due to its nontoxicity. In addition, the use of thermal stabilizers for the synthesis is not required [9–13].

In a previous work [2] these nano-structured PEDs already showed a much more improved dynamic mechanical behaviour than the medical-grade polyurethane (Pellethane®) at high number of cyclic loadings. In order to enhance the short- and long-term

* Corresponding author.
E-mail address: altstaedt@uni-bayreuth.de (V. Altstädt).

0032-3861/$ – see front matter © 2009 Elsevier Ltd. All rights reserved.
doi:10.1016/j.polymer.2009.09.051

mechanical behaviour of PEDs through stiffening of the material, an additional cross-linked network structure was introduced. The cross-linking can be achieved by using e-beam irradiation which promotes cross-linking among polymer chains [10]. The use of e-beam irradiation improves the static mechanical behaviour of polymers, but can also yield better dynamic creep and fatigue resistance [14].

This work focuses on the dynamic creep and fatigue behaviour of these novel nano-structured PEDs modified with various dosages of e-beam irradiation. Differential scanning calorimetry (DSC) was used to evaluate the thermal behaviour of the materials, and to identify any detrimental onset of material degradation. This method allows one to predict the extent of cross-linking that can be introduced to the material. Quasi-static tensile testing was performed to determine the ultimate strength of the PEDs, which is necessary for the dynamic SILT methodology and the evaluation of the dynamic creep behaviour measured by single load tests. In addition, atomic force microscopy (AFM) was carried out to highlight the micro-structure of the materials. The impact of e-beam irradiation on the mechanical properties of PEDs is discussed.

2. Experimental

2.1. Materials

The materials were segmented poly(aliphatic/aromatic-ester) (PED) multiblock copolymers containing poly(butylene terephthalate) (PBT) sequences which are extended with butylene ester of dilinoleic acid (DLA). DLA belongs to the group of dimer fatty acids. The semi-crystalline PBT is the hard segment phase while DLA is an amorphous diacid, which imparts the elastomeric characteristic to the polymer and therefore represents the soft phase segments. The biocompatibility of PBT and DLA has been well established and both can be used as a biomaterial or as blend components [8]. The chemical structure of the segmented PED is shown in Fig. 1.

In this study, two hard/soft segment ratios of PED were investigated (PBT-26 and PBT-30). PBT-26 contains 26 wt.% PBT and 74 wt.% DLA. PBT-30 respectively contains 30 wt.% PBT and 70 wt.% DLA, respectively. Pellethane®, which belongs to the thermoplastic polyurethanes (TPU) and a chemically cross-linked medical-grade silicone were used as benchmark materials for comparison of the PED copolymers with commercial products.

2.2. Sample preparation

Segmented multiblock copolymers (PED) were obtained in a two-stage process of transesterification and polycondensation in the melt as described elsewhere [15]. Briefly, dimethyl terephthalate (DMT) and 1,4-butanediol (1,4-BD) were subjected to transesterfication process to produce oligomer of butylene terephthalate (PBT) and using tetrabutoxy titanate as a catalyst. Then, oligomers of PBT were reacted with dimer fatty acid (here a dilinoleic acid, DLA) and a catalyst to initiate the polycondensation process at 250 °C. Hot reaction mass was extruded into water using compressed nitrogen, granulated and then purified by Soxhlet extraction from methanol [9,16].

In the next step, the materials were compression-moulded and e-beam irradiated. A linear electron accelerator Elektronika 10/10 was used to generate a 10 MeV electron beam for different dosages. The samples did not show any water uptake at standard laboratory conditions. Finally, micro dumbbells were produced from the material with a cutting tool according to DIN 53504 [17]. Puskas et al. [18] showed that the use of micro dumbbells is sufficient to monitor the fatigue performance of TPEs. Table 1 shows the materials of this study and the weight and number average molecular weight (M_n and M_W), the polydispersity index P_i, the intrinsic viscosity number η and the hardness.

2.3. Differential scanning calorimetry

Differential scanning calorimetry (DSC) scans of PED copolymers were performed using a DSC-Q1000 (TA Instruments, USA), with a triple cycle of heating–cooling–heating over the temperature range of −150 to 250 °C at a heating/cooling rate of 10 °C/min. The first heating cycle started at 23 °C and is intended to remove the thermal history. All DSC measurements were conducted in a nitrogen environment at a flow rate of 50 ml/min.

The glass transition temperature T_g of soft segments was determined from the upper inflection point of the received DSC thermogram. The crystallization temperature T_c was determined using the exothermic peak during the cooling cycle, while the melting temperature T_{m2} corresponds to the endothermic peak shown in the second heating cycle. In addition, the melting enthalpy ΔH_{m2} of PBT and the mass content of PBT crystallites $w_{c,h}$ were calculated [19–21].

2.4. Quasi-static testing

Tensile tests were carried out using a Zwick Z2.5 universal test equipment with a 0.5 kN load cell, a cross-head speed of 100 mm/min and a grip distance of 20 mm. The measurements were performed using sandpaper which was attached to the clamps in order to prevent slippage of the soft tensile bars from the clamps.

Tensile tests were performed with the benchmark materials as received under the standard laboratory conditions. The ultimate tensile stress σ_{max}, the elongation at break ε_{max} and Young's modulus E_{mod} were evaluated according to DIN 53504 [17]. The modulus of elasticity E_{mod} was calculated at 10% strain and all tensile results were averaged from 5 samples.

2.5. Fatigue testing

In order to conduct the hysteresis measurements, a servo-hydraulic test machine with a 20 kN servo cylinder, a 50 N load cell, a proper digital controller (Instron 8400/8800) and a special software package were used for the evaluation of the hysteresis loops. The resulting strain was measured using the real-time displacement between the specimen fixtures.

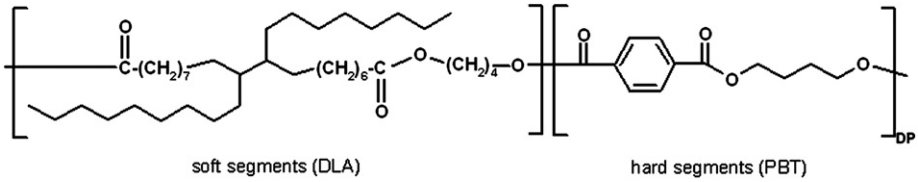

Fig. 1. Chemical structure of poly(aliphatic/aromatic-ester) (PED) multiblock copolymers, composed of dilinoleic acid (DLA) as the soft segments and poly(butylene terephthalate) (PBT) representing the hard segments.

Table 1
Physical properties of synthesized and e-beam irradiated poly(aliphatic/aromatic-ester) (PED) multiblock copolymers.

Designation	w_h (wt.%)	w_s (wt.%)	Additive	M_N (g/mol)	M_W (g/mol)	P_i	[η] (dL/g)	Hardness [Sh A]
PBT-26	26	74	–	4346	8854	2.04	0.79	68 A
PBT-30	30	70	–	5556	12,610	2.27	1.00	79 A
Silicone[a]	–	–	–	–	–	–	–	50 A
TPU	[a]	[a]	[a]	5986	9075	1.516	2.30	80 A

[a] No data available.

Fig. 2 presents the experimental setup. The hysteresis loops are continuously digitalized and the mid-curve of each hysteresis loop was subsequently calculated by the software package. Using this methodology it is possible to determine strain-, stiffness- and energy-related properties even for a non-linear viscoelastic behaviour. Beside small changes in material damping, small changes of the stiffness related parameters can be measured and used as damage criterion.

The step-wise increasing load test (SILT) was adopted for the hysteresis methodology in order to accelerate fatigue failure of the materials, by increasing step-wise the stress level using a single sample [6]. The initial dynamic load was 5% of the ultimate tensile stress as determined from static tensile testing following the work of El Fray [2,22,23]. During the fatigue testing, the dynamic load was increased by 5% after each interval of 1000 cycles, while maintaining a constant load ratio $R = \sigma_{min}/\sigma_{max} = 0.1$. The frequency varied between 1 Hz and 4 Hz corresponding to the frequency range of the movement of a human body [24–27]. The step-wise load function is shown in Fig. 3. The selected R value was used to maintain a tensile state of stress in the material during testing.

Moreover, a critical load level was determined using the SILT methodology. If the dynamic modulus E_{dyn}, which is related to the slope of the hysteresis loop, decreased up to 5% within one single load level, the critical value was reached. After determining the critical load values using the SILT methodology, the specimens were subjected to a stress controlled sinusoidal oscillation with a constant R value of 0.1 to maintain permanent tensile stress during cyclic loading. In addition, the stress was held constant during a period of 100,000 cycles. The adopted frequency of the cyclic loading was 1 Hz and no hysteretic heating was detected. This long-term testing methodology is called the single loading test (SLT) and was used in order to monitor the dynamic creep behaviour of the investigated materials [6].

2.6. Morphology characterization

2.6.1. TEM-microscopy

PBT-26 and PBT-30 samples were cut using a cryomicrotome into thin sections, which were subsequently stained with an aqueous solution of 0.2 wt.% osmium tetraoxide (OsO_4) at room temperature. Staining of the material was intended to affect the amorphous soft phase which appears as the dark phase because of the reaction of DLA with OsO_4 [28,29].

2.6.2. Atomic force microscopy (AFM)

A Dimension™ 3100 M (Metrology) atomic force microscope (Veeco/Digital Instruments) was used. Images with a size of $1 \times 1\ \mu m^2$ were acquired in tapping mode for all samples. The resolution was set to 512×512 points. The subsequent image processing includes image flattening using the software package Nanoscope 6.12r1.

3. Results and discussion

3.1. Differential scanning calorimetry (DSC)

Table 2 summarizes the thermal properties of PBT-26 and PBT-30. The glass transition temperature T_{g1} is only moderately influenced by the content of the hard phase. However, the increase in T_c and ΔH_{m2} for PBT-30 is caused by the larger concentration of the crystalline phase. In addition, the calculated degree of crystallinity $w_{c,h}$ is rather low (6.9–8.7%).

The T_{g1} only decreases with increasing dosage of irradiation for PBT-26, but not for PBT-30, but with respect to the standard deviation these changes are negligible. Irradiation influences the T_{g2} values, but significant differences can be seen for PED-26, where T_{g2} decreases from $57.3 \pm 0.6\ ^\circ C$ for the unirradiated material, to

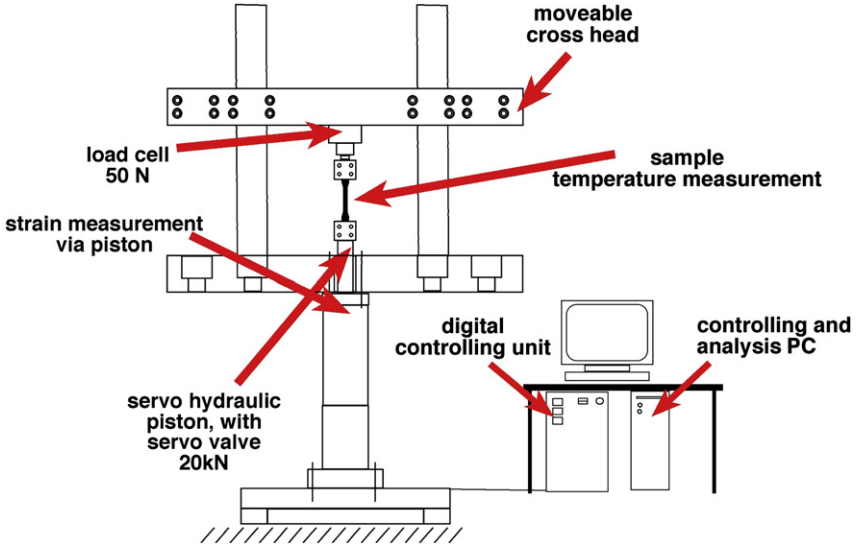

Fig. 2. Scheme of the experimental setup for the hysteresis measurement methodology [2].

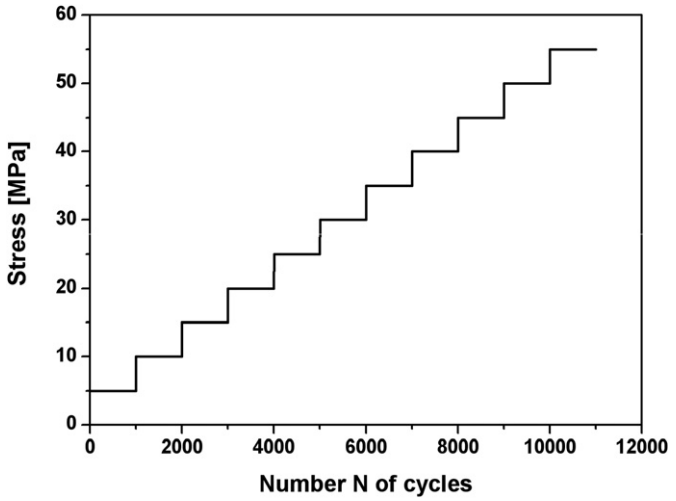

Fig. 3. Loading pattern as a function of the number N of cycles for the step-wise increasing load test (SILT) methodology. The stress amplitude was incrementally increased in steps of 5% of the ultimate tensile strength after each interval of 1000 cycles.

around 50–51.1 °C, for the irradiated specimens, what can be explained by the effect of the lack of a strong segmental interactions stabilizing the nanostructure at the molecular level. A similar effect is visible for the crystallinity, which only is significantly decreasing for irradiated PBT-26 compared to neat PBT-26. These results indicate that cross-linking predominantly occurs in the hard PBT phase, rather than in the soft DLA segment. With increasing radiation dose, the random polymer structure may favour formation of longer PBT segments to initiate more entanglements and hence requires more thermal agitation to achieve the glass transition. Therefore, the degree of crystallinity is also reduced. For polymers containing 30 wt.% hard segments, e-beam irradiation slightly increases T_{m2} of PBT. This trend does not apply to all results in Table 2, since e-beam irradiation does not only initiate cross-linking, but also cause polymer chain scission and material degradation. In addition, the use of e-beam irradiation does not affect the crystallization behaviour of PBT as indicated by the inconsiderable change of T_c in Table 2.

3.2. Quasi-static testing

Screening of the material mechanical behaviour was performed in order to study how e-beam irradiation and the formation of the network structure affect the tensile properties. Table 3 presents the results for E_{mod}, σ_{max} and ε_{max}. Comparing the neat materials, an overall improvement in the mechanical behaviour (σ_{max} and ε_{max}) can be observed with increasing fraction of the hard phase. The increase of ε_{max} can be related to the micro-structure of the polymer, since the higher soft-phase content of PBT-26 yields a more homogeneous structure than the microphase separated structure of PBT-30 [8]. In addition, PBT-30 is stiffer than PBT-26, since Young's modulus increases from 7.7 MPa to 13.5 MPa (Table 3). These results reveal the favourable contribution of a higher concentration of the hard phase (PBT) to enhance the mechanical response of the material as it is generally accepted for thermoplastic elastomers (the stiffness increases with content of hard segments [1]).

Fig. 4 shows the stress–strain curves of the polymers used within this study. Both, PBT-26 and PBT-30 have a relatively high elongation at break, which can be related to the long chain aliphatic DLA segments, used as the soft phase within the TPEs. In addition, the PEDs do not depict a typical rubber-like behaviour similar to the benchmark materials silicone and TPU, which are characterized by a chemical (silicone) or a physical network structure reinforced with hydrogen bonding (TPU). The presence of additional hydrogen bonds in the TPU is responsible for the high tensile strength, whereas different hardening additives are responsible for the tensile strength of silicone. We emphasize that synthesized PED copolymers do not contain any additives or even thermal stabilizers, and still display very good mechanical properties [8].

Table 3 and Fig. 4 show that the use of e-beam irradiation and the amount of irradiation dosage increases σ_{max} and ε_{max} of the materials via the formation of the cross-linked network structure. E-beam irradiation has only a minor effect on E_{mod} of PBT-26 (see Table 3) and PBT-30 (see also Fig. 4).

E-beam irradiation essentially creates free radicals along the polymer chains. These free radicals can be re-combined to form cross-links [30]. However, the resulting free radicals can also react with the oxygen bi-radicals which leads to oxidation and other related free radical reactions. This effect can cause polymer chain scission and material degradation [30]. The onset of material degradation explains the drastic drop in σ_{max} and ε_{max} of TPU (see Table 3) and the colour change (yellowing) of the material with various dosages of e-beam irradiation.

Because of possible e-beam induced degradation, α-tocopherol was added for stabilization of the PED copolymers [31–33]. The tensile curves of original and modified PBT-26 in Fig. 5 show that the use of α-tocopherol as a stabilizer does not affect the mechanical tensile performance. Even e-beam irradiation does not change the tensile properties of PBT-26 modified with α-tocopherol [34].

3.3. Fatigue testing

The tensile strength σ_{max} is a necessary parameter for calculating the different loading steps in the fatigue measurements. Fig. 6 presents the σ_{max} values for PBT-26 and PBT-30. PBT-26 as well as PBT-30 have an increased tensile strength, resulting from

Table 2
Temperature transitions determined with differential scanning calorimetry for PBT-26 and PBT-30 with and without e-beam irradiation.

Sample	Soft segments	Hard segments				
	T_{g1} [°C]	T_{g2} [°C]	T_{m2} [°C]	ΔH_{m2} [J/g]	T_{c2} [°C]	$w_{c,h}$ [%]
PBT-26 (0 kGy)	−43.7 ± 0.3	57.3 ± 0.6	115.1 ± 0.4	8.9 ± 0.2	27.4 ± 0.5	6.9 ± 0.2
PBT-26 (25 kGy)	−43.9 ± 0.2	49.9 ± 0.4	114.1 ± 0.5	9.2 ± 0.1	22.4 ± 0.2	5.8 ± 0.3
PBT-26 (50 kGy)	−43.6 ± 0.3	51.1 ± 0.6	114.1 ± 0.2	9.1 ± 0.2	22.9 ± 0.6	6.2 ± 0.3
PBT-26 (75 kGy)	−43.6 ± 0.4	50.3 ± 0.3	114.5 ± 0.5	6.6 ± 0.3	22.3 ± 0.3	5.8 ± 0.2
PBT-26 (100 kGy)	−43.0 ± 0.1	50.0 ± 0.3	114.2 ± 0.4	8.0 ± 0.3	22.5 ± 0.2	5.8 ± 0.4
PBT-30 (0 kGy)	−42.6 ± 0.1	49.0 ± 0.4	124.1 ± 0.4	8.7 ± 0.4	52.1 ± 0.4	8.4 ± 0.4
PBT-30 (25 kGy)	−41.9 ± 0.4	50.3 ± 0.2	128.3 ± 0.4	9.2 ± 0.4	52.3 ± 0.4	8.2 ± 0.4
PBT-30 (50 kGy)	−42.5 ± 0.3	50.5 ± 0.3	125.2 ± 0.4	9.7 ± 0.4	51.3 ± 0.4	8.3 ± 0.4
PBT-30 (75 kGy)	−42.1 ± 0.3	49.5 ± 0.4	124.2 ± 0.4	10.2 ± 0.4	52.4 ± 0.4	8.7 ± 0.4
PBT-30 (100 kGy)	−41.9 ± 0.2	50.7 ± 0.4	126.2 ± 0.4	9.9 ± 0.4	52.4 ± 0.4	8.2 ± 0.4

Table 3
Static tensile properties of PEDs, TPU and silicone. The geometry of the samples was chosen according to DIN 53504 [17]. The cross-head speed was 100 mm/min. The ultimate tensile strength is denoted by σ_{max}, the elongation at break by ε_{max} and Young's modulus by E.

Sample	E [MPa]	σ_{max} [MPa]	ε_{max} [%]
PBT-26			
0	7.7 ± 0.2	3.8 ± 0.1	512 ± 17
25	8.4 ± 0.8	4.0 ± 0.2	563 ± 101
50	8.3 ± 0.1	3.9 ± 0.1	580 ± 50
75	8.0 ± 1.1	4.3 ± 0.2	534 ± 87
100	7.7 ± 0.5	4.7 ± 0.3	832 ± 92
PBT-30			
0	13.5 ± 0.7	6.1 ± 0.2	790 ± 30
25	13.6 ± 0.1	6.6 ± 0.3	838 ± 76
50	13.9 ± 0.4	7.4 ± 0.2	901 ± 10
75	14.1 ± 0.3	7.2 ± 0.2	790 ± 80
100	13.1 ± 0.3	7.3 ± 0.3	895 ± 50
PBT-26 α[a]			
0	7.2 ± 0.3	4.0 ± 0.2	607 ± 28
25	7.0 ± 0.3	3.6 ± 0.1	447 ± 68
50	7.8 ± 0.4	4.1 ± 0.2	657 ± 81
75	8.0 ± 0.2	4.0 ± 0.1	659 ± 53
100	7.5 ± 0.3	4.0 ± 0.1	620 ± 47
PBT-30 α[a]			
0	12.5 ± 0.8	5.6 ± 0.1	664 ± 25
25	13.1 ± 0.8	5.8 ± 0.2	722 ± 76
50	13.5 ± 0.7	6.5 ± 0.4	790 ± 102
75	12.3 ± 0.7	5.8 ± 0.3	690 ± 51
100	12.4 ± 0.3	5.6 ± 0.2	597 ± 69
TPU			
0	26.4 ± 0.3	52.9 ± 4.8	910 ± 21
25	26.9 ± 0.5	42.4 ± 1.2	891 ± 86
50	_[b]	_[b]	_[b]
75	25.3 ± 1.3	32.6 ± 5.2	786 ± 129
100	_[b]	_[b]	_[b]
Silicone			
	2.3 ± 0.2	10.2 ± 0.8	1034 ± 91

[a] α = α-Tocopherol.
[b] No useable results were obtained, due to slippage of the tensile bars during testing.

the e-beam irradiation dosage of 50 kGy and therefore are taken for further investigations.

Fig. 7 provides the dynamic modulus E_{dyn} results during the SILT of TPU, neat PBT-26 and PBT-30 and both irradiated with a dosage of

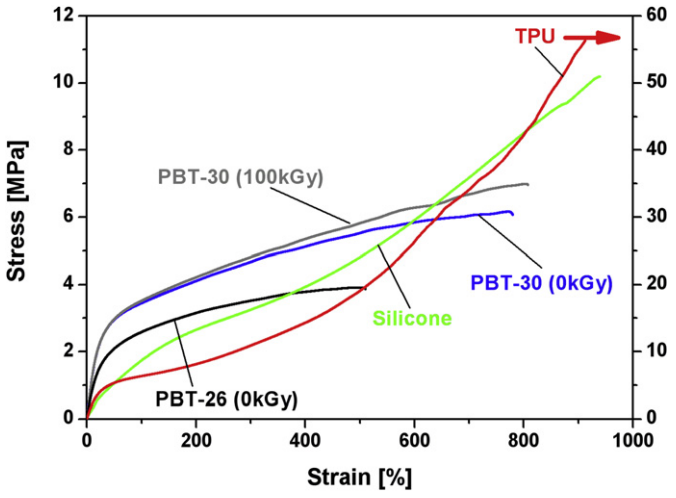

Fig. 4. Stress–strain tensile curve of PBT-26, PBT-30 with 0 kGy and 100 kGy of e-beam irradiation, silicone and TPU. The measurements were performed on 1 mm thin films with a cross-head speed of 100 mm/min.

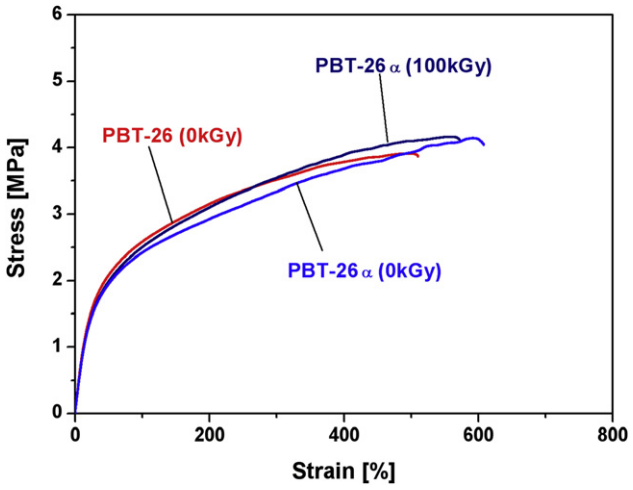

Fig. 5. Stress–strain tensile curve of PBT-26, PBT-26$_{\alpha 0kGy}$ and PBT-26$_{\alpha 100kGy}$. The measurements were performed on 1 mm thin films with cross-head speed of 100 mm/min.

50 kGy. For PBT-26 and PBT-30 systems, the dynamic E_{dyn} is higher than the static values ($E_{mod}^{PBT-26} = 7.7$ MPa, $E_{mod}^{PBT-26_{50kGy}} = 8.3$ MPa, $E_{mod}^{PBT-30} = 13.5$ MPa, $E_{mod}^{PBT-30_{50kGy}} = 13.9$ MPa), which can be related to the viscoelastic response of the material to the higher loading velocity during dynamic loading than during quasi-static testing.

Fig. 7 reveals that the neat PBT-26 has a lower E_{dyn} than the commercial TPU. However after the 5th load level (5000 cycles), the neat PBT-26 even exhibits a higher dynamic modulus and does not depict from such a drastic drop like TPU. Polyurethane samples generally show higher initial E_{dyn} values, which drop faster with increasing load levels [23,35]. Takahara et al. suggested that under cyclic loading the destruction of the hard segment domain or a mixing of the hard and soft segment occurs [36,37]. Therefore PBT-26 is more resistant to fatigue than TPU. Comparison of irradiated PBT-26 reflects that at low stress levels, the irradiated PBT-26 has an improved dynamical performance, which is comparable to commercial TPU. Similar to the neat PBT-26, the irradiated material shows no drastic drop of E_{dyn} and outperforms TPU after 3000 cycles. This positive effect is related to the cross-linking due to e-beam irradiation, which introduces additional chemical bonds

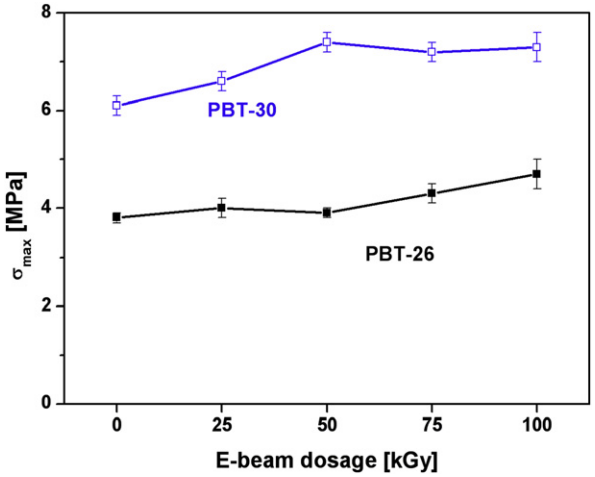

Fig. 6. Ultimate tensile strength (σ_{max}) of the neat and irradiated PBT-26 and PBT-30.

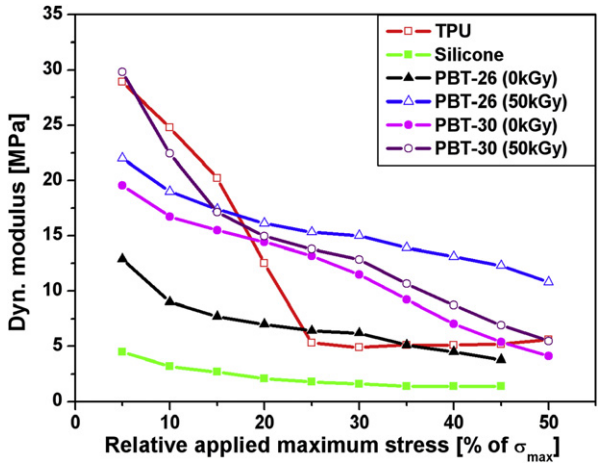

Fig. 7. Dynamic modulus E_{dyn} as a function of relative applied maximum stress for silicone, TPU, neat PBT-26, PBT-26$_{50kGy}$, neat PBT-30 and PBT-30$_{50kGy}$ (SILT).

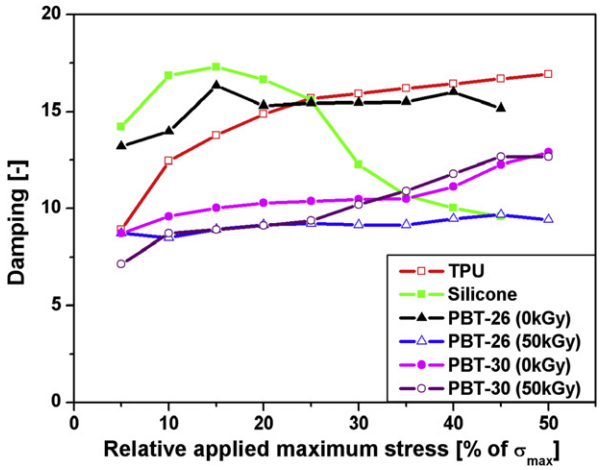

Fig. 9. Damping versus number N of cycles for silicone, TPU, neat PBT-26, PBT-26$_{50kGy}$, neat PBT-30 and PBT-30$_{50kGy}$ (SILT).

between the backbone chains to stiffen the material. As expected for PBT-30 the dynamic modulus E_{dyn} is increased compared to PBT-26 because of the higher amount of the PBT hard phase. Irradiation of PBT-30 causes an increase of E_{dyn}, similar to commercial TPU. During the first two loading levels, E_{dyn} strongly drops. Similar to TPU this drop can be related to the destruction of the hard segment domains. As this drop does not occur within the neat PBT-30 this effect can be explained by the formation of cross-links. DSC measurements already indicated that these cross-links are predominantly in the PBT hard phase. Furthermore, it is obvious that irradiated PBT-26 has a much lower deformation at the same loading level than the neat material and commercial TPU (see Fig. 8). A similar effect can be observed for the neat and irradiated PBT-30. The lower the soft-phase content, the lower is the susceptibility to dynamic creep [22]. Therefore the reduction of the deformation during the dynamic loading of the SILT methodology, due to e-beam irradiation is not as pronounced as for PBT-26.

When the microdomains are destroyed, TPU creeps more severely within each loading level. Hence, the neat PBT-26 is also more susceptible to creep than PBT-26$_{50kGy}$. This also holds for PBT-30. The chains of the irradiated PED have lesser possibilities to slide against one another, due to the formation of cross-links and lower amount of energy is dissipated by hysteretic heating, which is caused by the friction of polymer chains against each other [38].

A review of the damping characteristics of the materials during SILT also underlines that e-beam irradiation enhances the dynamic performance of the PED (see Fig. 9). The damping is defined as the area, which is covered by a hysteresis loop [7]. A higher damping is related to higher loss of energy. The energy can be dissipated due to hysteretic heating and the formation of micro cracks, which creates new surfaces [39]. PBT-26 shows the highest damping value followed by neat PBT-30. This behaviour indicates, that at such compositions (only 26 wt.% of hard segments), the material creeps due to the missing of strong segmental interactions, to stabilize the nanostructure at the molecular level. Therefore, a highly homogeneous rather than a microphase separated structure is expected for these polymers. The difference between PBT-26 and PBT-30 indicates that the structure of PBT-26 is even more homogeneous than the structure of PBT-30. Both irradiated polymers show a decreased value of damping which can be explained by the formation of a higher degree of microphase separation due to e-beam irradiation. Hence, e-beam irradiation improves the fatigue resistance of the multiblock polyester copolymers especially for lower loading cycles by reducing the damping. Because of the additional cross-

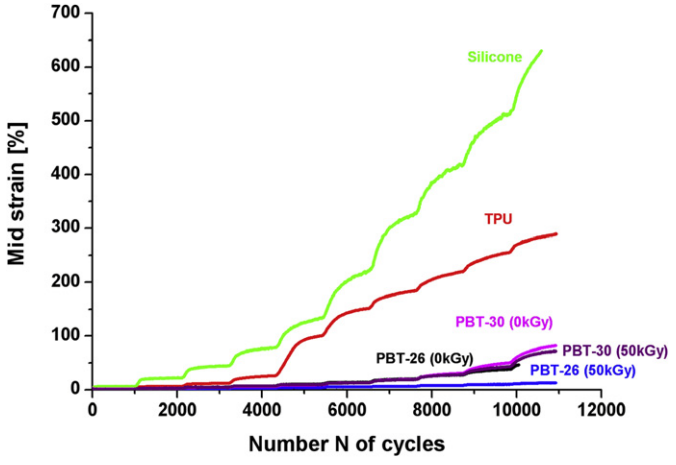

Fig. 8. Mid-strain as a function of number N of cycles for silicone, TPU, neat PBT-26, PBT-26$_{50kGy}$, neat PBT-30 and PBT-30$_{50kGy}$ (SILT).

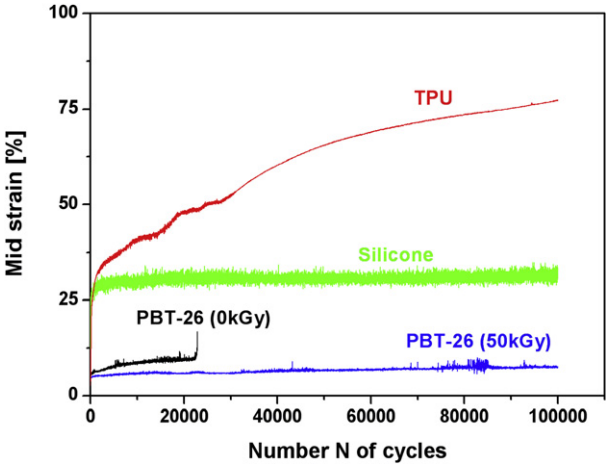

Fig. 10. Dynamic creep for silicone, TPU, neat PBT-26, PBT-26$_{50kGy}$, neat PBT-30 and PBT-30$_{50kGy}$ measured by the single load test (SLT) methodology. The test frequency was 1 Hz, the number of cycles N was 100,000 and $T = 24\,^{\circ}C$.

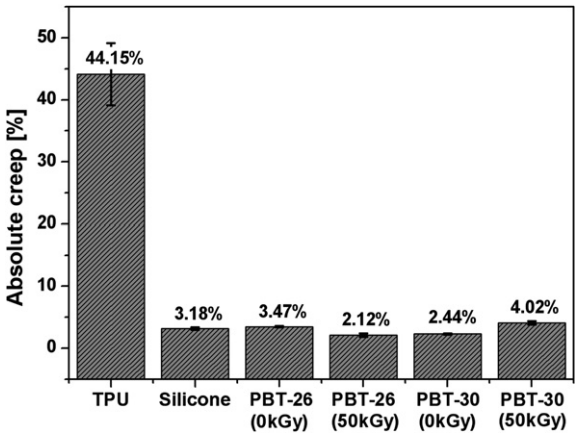

Fig. 11. Absolute creep $\Delta\varepsilon$ of PED copolymers, silicone and TPU. The test parameters were: frequency = 1 Hz, number of cycles $N = 100{,}000$ and $T = 24\,^{\circ}C$.

links, more bonds have to be broken to create cracks for energy dissipation. For all loading levels, PBT-26_{50kGy} exhibits nearly the same damping behaviour, whereas the TPU has a notable increasing damping value after each load level. Both neat and irradiated PEDs show a mild increasing trend in damping.

Analyzing the data of Fig. 7 the critical load level is set at the 4th load level. In this interval, E_{dyn} drops more than 5% within one loading level. For the following SLT measurements the appropriate load is applied and Fig. 10 shows the results for different material systems.

Non-irradiated PBT-26 already breaks after around 22 000 cycles, while irradiated PBT-26 sustains the loading conditions up to 100,000 cycles. This is consistent with the SILT results, where the non-irradiated PBT-26 also does not sustain all load levels. A pronounced creep of the segmented TPU system is visible over 100,000 cycles. The different steps can be explained by the destruction of the microdomains [40]. In the PBT materials these domains are not destroyed. Consequently the PBT material is less sensitive to dynamic creep than the TPU system and the silicone, see Fig. 11.

The irradiated PBT-26 shows a lower susceptibility to dynamic creep than the neat polymer and even lower than all other materials. This decrease of the absolute creep is related to the formation of cross-links due to e-beam irradiation. By introducing an additional network, a stable polymer structure is formed. During the dynamic loading the number of entanglements decreases and the chemical bonds are responsible for carrying the load. Since more chemical bonds have to break before the sample fails, the irradiated PBT-26 sustains the whole loading pattern while PBT-26 breaks at a smaller number of cycles (see Fig. 10). Due to the double physical and chemical network structure the final elongation of the sample is also decreased and the dynamic creep behaviour is improved. In comparison, the neat PBT-30 sustains all loading cycles without breakage as well as irradiated PBT-30. Its absolute creep is smaller than the absolute creep for the neat and irradiated PBT-26, which indicates that with lower soft-phase content the susceptibility to creep is also smaller [22]. In addition, the absolute creep of neat PBT-30 is smaller than for irradiated PBT-30. This result underlines the conclusion that cross-linking mainly occurs in the PBT hard phase. In comparison to PBT-26 a dosage of 50 kGy is not sufficient to improve the dynamic creep behaviour of PBT-30. It is worthwhile to mention, that the applied loading level during the SLT of irradiated PBT-30 is slightly higher than for the non-irradiated PBT-30, while the applied loads were nearly equal for PBT-26 (see Fig. 6). Therefore it is reasonable, that irradiated PBT-30 has a slightly higher absolute creep value than the non-irradiated one. In addition, no destruction of the micro-structure is visible because no steps or a rapid growth during the strain measurements can be detected, similar to the SLT of PBT-26.

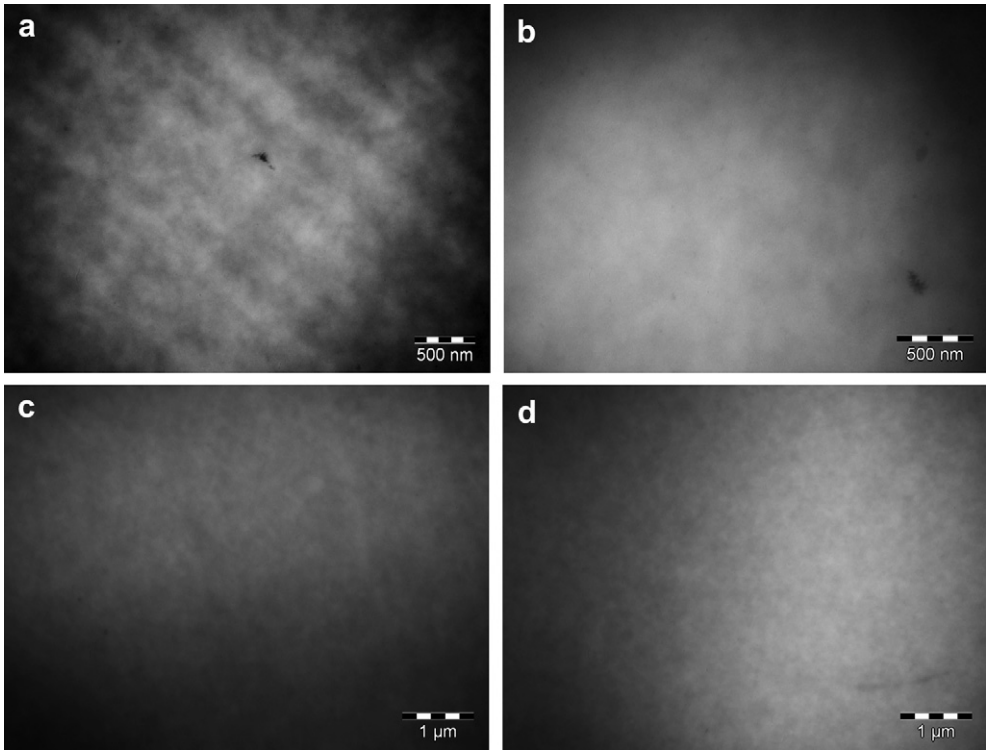

Fig. 12. Transmission electron micrographs (TEMs) of PBT-26_{0kGy} (a), PBT-26_{100kGy} (b) PBT-30_{0kGy} (c) PBT-30_{100kGy} (d). The samples were stained using vapour from a 0.2 wt.% aqueous OsO_4 solution for two hours at room temperature.

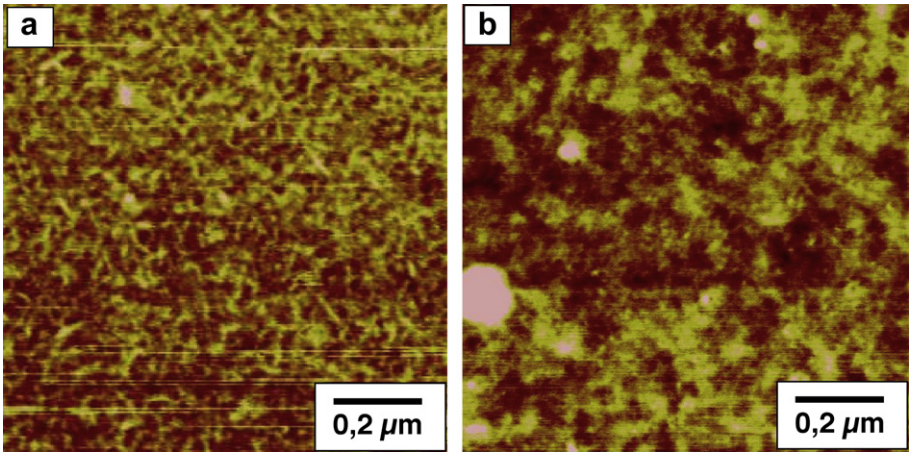

Fig. 13. Two-dimensional atomic force micrographs (AFM) of PBT-30_{0kGy} (a) and PBT-30_{50kGy} (b). Images with a size of $1 \times 1\ \mu m^2$ were acquired in tapping mode.

3.4. Morphology characterization

Fig. 12 shows the micro-structure of PBT-26 and PBT-30 for non-irradiated and irradiated samples. The bright phase is related to the PBT hard phase, whereas the dark phase belongs to the DLA soft phase, which reacts with OsO_4. Fig. 13 presents the TEM images for PBT-26 and PBT-30. In the non-irradiated sample the phase separation is visible, which is responsible for the strength of the polymer [8]. Different resolutions of TEM images of PBT-26 and PBT-30 are shown, because of the difficulties to stain the samples.

The TEM images reveal that phase separation is reduced with increasing dosage of irradiation. The larger amount of the bright phase shows that this can be related to the formation of a cross-linked network structure. Phase transitions occur predominantly in hard segments, therefore white phase is related to hard PBT segments. A similar trend holds for PBT-30 (see Fig. 12). It is reported that at higher soft-phase contents (i.e. 74 wt.%) a more homogeneous structure than the microphase separated structure like PBT-30 (with 70 wt.% soft segments) exists [8]. This effect is visible by comparing PBT-26 and PBT-30. It is worthwhile mentioning that the straight, dark and light regions in Fig. 12(b) result from sectioning of the samples and do not reflect or belong to the micro-structure of this material. In order to investigate the micro-structure of the PED polymers in more detail AFM measurements were applied, because TEM only showed the reported effects very unincisive. The AFM images of the two extreme, PBT-30_{0kGy} and PBT-30_{100kGy} reveal the influence of e-beam radiation on the polymers (Fig. 13).

Phase separation results in hard phase domains (bright) and soft phase domains (dark). The neat polymer shows a well ordered structure of hard phase domains. In comparison the irradiated polymer has larger bright domains, which look like agglomerations of the bright phase. This effect can be related to the e-beam irradiation, which takes place after the polymerisation and introduces cross-links into the copolymer. In addition, the samples are slightly heated during the irradiation process. Therefore, larger connected domains can undergo room temperature annealing and agglomerate, because of the enhanced micro-mobility of the polymer chains at higher temperatures [1,39] and increases the amount of phase separation. These results also reinforce the statement, that the cross-linking predominantly occurs between the hard phase, see the discussion of the DSC results. Finally, the improved fatigue behaviour can be related to the micro-structure as well as the increase of the ultimate tensile strength. Furthermore, that e-beam irradiation randomly breaks and reconnects bonds within the polymer [34]. Hence the micro-structure of the irradiated polymer consists of large interconnected domains while, the neat polymer has a more regular structure.

4. Conclusion

The dynamic creep and fatigue performance of novel nano-structured poly(aliphatic/aromatic-ester) multiblock copolymers (PEDs) with various dosages of e-beam irradiation were investigated. DSC measurements indicated that cross-linking mainly occurs within the PBT hard phase, shown by the slight increase of T_{m2} and the decrease of the crystallinity. It was found that the introduction of the additional network influences the micro-structure. For PED, the increase of irradiation dosage leads to the formation of PBT hard phase agglomerations, which has a reinforcement effect on the material. This formation of an additional cross-linked network in the polymer is responsible for improving the quasi-static mechanical properties of these PED multiblock copolymers.

As expected, the improvement in the mechanical performance was also observed in the fatigue and creep behaviour of irradiated PEDs compared to the neat PEDs, TPU and silicone. Particularly the irradiated materials, show a less drastic drop of E_{dyn}, as compared to TPU and were more resistant to creep. In addition, the irradiated PEDs were more resilient against micro-scale damage to lower damping. Therefore, thermoplastic elastomers, especially PED multiblock copolymers can be considered as good candidates for medical applications, where materials are subjected to oscillatory deformations.

Acknowledgments

The authors are grateful to the Deutsche Forschungsgemeinschaft and the Polish Ministry of Science and Higher Education for financial support (DFG-Project Al 474/12-1 and DWM/18/POL/2005).

References

[1] Holden G, Legge NR, Quirk N, Schroeder HE. Thermoplastic elastomers. 3rd ed. Munich: Hanser Publishers; 1996.
[2] El Fray M, Altstädt V. Polymer 2003;44:4635–42.
[3] Szycher M. Polyurethane elastomers in medicine. New York: Marcel Dekker; 1990.
[4] Bakker D, van Blitterswijk CA, Hesseling SC, Koerte HK, Kuijpers W, Grote JJ. J Biomed Mater Res 1990;24:489–515.
[5] Wise DL. Biomaterial and bioengineering handbook. New York: Marcel Dekker; 2000.
[6] Raue F, Ehrenstein GW. Macromol Symp 1999;148:229–40.

[7] Altstädt V. Hysteresismessungen zur charakterisierung der mechanisch–dynamischen eigenschaften von R-SMC. PhD dissertation, University Kassel; 1987.
[8] El Fray M. Nanostructured elastomeric biomaterials for soft tissue reconstruction. Warszawa: Publishing House of the Warsaw University of Technology; 2003. p. 1–144.
[9] El Fray M, Slonecki J. Angew Makromol Chem 1996;234:103–9.
[10] El Fray M, Bartkowiak A, Prowans A, Slonecki J. J Mater Sci Mater Med 2000;11:757–62.
[11] Prowans P, El Fray M, Slonecki J. Biomaterials 2002;23(14):2973–8.
[12] Renke-Gluszko M, El Fray M. Biomaterials 2004;25(21):5191–8.
[13] El Fray M, Prowans P. Institute of Organic and Polymer Technology (Wroclaw). Sci Papers 2003;52:481–4.
[14] Rouif S. Nucl Instrum Meth B 2005;236:68–72.
[15] Fakirow S. Handbook of condensation thermoplastic elastomers. Weinheim: Wiley-VHC Verlag GmbH & Co. KGaA; 2005.
[16] El Fray M, Slonecki J. Polish Patent PL. 308 185; 2000.
[17] Din Iso 53504. Determination of tensile stress/strain properties of rubber; 2005.
[18] Puskas JE, Dos Santos LM, Fischer F, Götz C, El Fray M, Altstädt M, et al. Polymer 2009;50:591–7.
[19] Hesketh TR, van Bogart JWC, Cooper SL. Polym Eng Sci 1980;20:190–7.
[20] Koberstein JT, Galambos AF, Leung LM. Macromolecules 1992;25:6195–204.
[21] Jimenez G, Asai S, Shishido A, Sumita M. Eur Polym J 2000;36:2039–50.
[22] El Fray M, Altstädt V. Polymer 2003;44:4643–50.
[23] El Fray M, Altstädt V. Polymer 2004;45:263–73.
[24] Schechtman H, Bader DL. Eng Med 1994;208:241–8.
[25] Schechtman H, Bader DL. J Biomech 1997;30:829–35.
[26] Bennet MB, Ker RF, Dimery NJ, Alexander RM. J Zool London 1986;209:537–48.
[27] Carlstedt CA, Nordin M. Biomechanics of tendons and ligaments. In: Nordin M, Frankel Vh, editors. Biomechanics of tissues and structures of musculoskeletal system, vol. 59. London: Lea & Febiger; 1980.
[28] Sawyer LC, Grubb D. Polymer microscopy. London: Chapman & Hall; 1996.
[29] El Fray M, Slonecki J. Angew Makromol Chem 1999;266:30–6.
[30] Grossman RF. Antioxidants, polymer modifiers and additives. Basel: Marcel Dekker; 2001.
[31] Packer L. Am J Clin Nutr 1991;53:1050–5.
[32] Packer L, Kagan VE. Vitamin E: the antioxidant harvesting center of membranes and lipoproteins. In: Packer L, Fuchs J, editors. Vitamin E in health and disease. New York: Marcel Dekker, Inc.; 1993.
[33] Burton G, Ingold K. J Am Chem Soc 1981;103:6472–7.
[34] Oral Ebru, Wannomae KK, Rowell SL, Kamil Muratoglu Orhun. Biomaterials 2006;27(11):2434–9.
[35] Oertel G. Polyurethane handbook. Munich: Hanser; 1985.
[36] Takahara A, Hamada K, Kajiyama T, Takayanagi M. J Biomed Mater Res 1985;19:13–34.
[37] Takahara A, Hamada K, Kajiyama T, Takayanagi M. J Biomed Mater Res 1985;26:987–96.
[38] Galetz MC, Goetz C, Adam P, Glatzel U. Adv Eng Mater 2007;9(12):1089–96.
[39] Grellmann W, Seidler S. Deformation and fracture behaviour of polymers. Heidelberg: Springer; 2001.
[40] Szycher M. Handbook of polyurethanes. Boca Raton, Florida: CRC Press Inc.; 1986.